

## Supplementary material

### Chemicals

Bulk 2H-MoSe<sub>2</sub> (single crystal) was purchased from HQ Graphene. In (99.9999 %, granules) and Se (99.9999 %, granules) powders were purchased from Wuhan Xinrong New Material Co., China. Tin (99.999 %, granules) and S (99.9999 %, granules) were purchased from Wuhan Xinrong New Material Co., China. SnCl<sub>2</sub> (99.9%) was supplied by Strem. Chemicals, USA. The solvents were supplied by Sigma Aldrich, the PTAA by Solaris (Mw =20–70 kDa), the PbI<sub>2</sub> and PbBr<sub>2</sub> by TCI America, the FAI (FA = formamidinium) and MABr (MA = methylammonium) by GreatCell Solar, the CsI and RbI by Sigma-Aldrich, the PC<sub>70</sub>BM ([6,6]-Phenyl-C71-butyric acid methyl ester) by Solenne, and bathocuproine (BCP) by Sigma-Aldrich. ITO substrates were acquired from Naranjo Substrates. All solvents and commercial reagents were used as received unless otherwise stated.

### Material synthesis, exfoliation, and characterization

Bulk SnS<sub>2</sub> was synthesized through direct synthesis from elements. Experimentally, Sn and S, in an amount corresponding to 20 g of SnS<sub>2</sub> were placed in quartz ampoule (35x200 mm) together with 1 at% excess of sulfur and 0.5 g of SnCl<sub>2</sub> and melt sealed under high vacuum ( $<1 \times 10^{-3}$  Pa using diffusion pump with LN2 trap) using oxygen-hydrogen torch. The ampoule was placed horizontally in a muffle furnace and heated at 450 °C for 25 h, and then at 500 °C, 600 °C and 800 °C for 50 h. Finally, the ampoule was placed in two zone furnace and source zone was heated at 600 °C while the growth zone was heated at 800 °C. After 2 days, the temperature gradient was reversed, and source zone was kept at 800 °C while growth zone was kept at 700 °C. After 10 days of growth, the ampoule was cooled down to room temperature and opened in Ar-filled glovebox.

β-InSe bulk crystals were produced through the modified Bridgman–Stockbarger method, adjusting the synthesis protocol described in ref <sup>1</sup>. The experimental procedure is detailed in ref <sup>2</sup>.

The investigated transition metal chalcogenides (TMCs), *i.e.*, MoSe<sub>2</sub>, SnS<sub>2</sub> and InSe, were exfoliated in form of nanosheets by means of ultrasonication-assisted liquid-phase exfoliation (LPE) <sup>3</sup> in anhydrous 2-propanol (IPA, 99.5%, Sigma Aldrich)<sup>2,4</sup>, followed by sedimentation-based separation (SBS) to remove unexfoliated material<sup>2,4</sup>. More in detail, 100 mg of bulk TMCs, previously powdered in a mortar, were added to 100 mL of anhydrous IPA and ultrasonicated in a bath sonicator (Branson® 5800 cleaner, Branson Ultrasonics) for 9 h. The resulting dispersions were ultracentrifuged at 2700 g (Optima™ XE-90 with a SW32Ti rotor, Beckman Coulter) for 20 min at 15 °C to separate unexfoliated bulk crystals (sediment) from the exfoliated materials (supernatant). Then, 80% of the supernatants were collected to obtain the final TMC dispersions. A solvent exchange approach was used to replace the anhydrous IPA with anhydrous chlorobenzene (CB). Experimentally, 2D TMC dispersions in anhydrous IPA were ultracentrifuged for 2 h to precipitate exfoliated materials. The anhydrous IPA was then removed by pipetting and, afterwards, anhydrous CB was added. The ultracentrifugation step was repeated, removing CB solvent which may still contain IPA residues. Lastly, anhydrous CB was added again to obtain the final dispersions with a concentration of ~1.0 mg mL<sup>-1</sup>.

Transmission electron spectroscopy (TEM) measurements of TMC nanosheets (deposited on ultrathin C-on-hole C-coated Cu grids) were performed with a JEM 1011 (JEOL) TEM (thermionic LaB<sub>6</sub> crystal), operating at 120 kV. The morphological and statistical analyses were performed by using ImageJ software (NIH) and OriginPro 9.1 software (OriginLab), respectively.

X-ray diffraction (XRD) measurements of TMC bulk and nanosheets (deposited on onto Si/SiO<sub>2</sub> substrates) were carried out with a PANalytical Empyrean using Cu K $\alpha$  radiation.

Raman spectroscopy measurements of the TMC nanosheets (deposited onto Au-coated Si/SiO<sub>2</sub> substrates) were performed with a Renishaw microRaman InVia 1000 mounting a 50 $\times$  objective, with an excitation wavelength of 633 nm and an incident power of 1 mW. For each sample, 50 spectra were collected.

### Device Fabrication

A thin film of PTAA was deposited from a  $2 \text{ mg mL}^{-1}$  solution on ITO substrates treated with UV-Ozone for 20 min, and then annealed at  $110 \text{ }^{\circ}\text{C}$  for 10 min. The quadruple cation perovskite precursors solution was prepared by dissolving 45.3 mg MABr, 394.7 mg FAI, 66.0 mg  $\text{PbBr}_2$ , 1266.4 mg  $\text{PbI}_2$  in 1.8 mL 4:1 vol./vol. anhydrous DMF:DMSO. Next, 114.2  $\mu\text{L}$  and 95.2  $\mu\text{L}$  of 1.5 M CsI and 1.5 M RbI stock solutions, respectively, were added in the perovskite precursors solution. The nominal composition of the quadruple perovskite was  $\text{Cs}_{0.05}\text{Rb}_{0.04}(\text{FA}_{0.85}\text{MA}_{0.15})_{0.91}\text{Pb}(\text{I}_{0.91}\text{Br}_{0.09})_3$ . The perovskite layer was dynamically spin-coated onto ITO/PTAA substrates at 6000 rpm for 45 s. At 20 s before the end of the spinning process, 200  $\mu\text{L}$  of anhydrous CB was dropped onto the spinning perovskite film. Subsequently, the samples were immediately annealed for 45 min on a pre-heated hotplate at  $100 \text{ }^{\circ}\text{C}$ . For the deposition of  $\text{MoSe}_2$ ,  $\text{SnS}_2$  and  $\text{InSe}$  nanosheets on the perovskite surface, 40  $\mu\text{L}$  of the corresponding dispersions were dynamically spin coated at 3000 rpm. Next, an approximately 30 nm-thick layer of  $\text{PC}_{70}\text{BM}$  was spin-coated from a  $20 \text{ mg mL}^{-1}$  solution in anhydrous CB at 2000 rpm for 60 s. Subsequently, BCP was spin-coated from a  $0.5 \text{ mg mL}^{-1}$  solution prepared in extra dry IPA at 4000 rpm for 45 s. Finally, a 100 nm-thick Ag top electrode was deposited by thermal evaporation under a high vacuum of  $10^{-6}$  mbar.

## Device Characterization

The valence band maximum (VB) energy position and the work function ( $W_F$ ) of the perovskite films were estimated by ambient photoemission spectroscopy (APS) using an APS04 N2-RH system (KP Technology). The contact potential difference (CPD) was measured utilizing a gold alloy vibrating probe (2 mm diameter). The absolute  $W_F$  of the tip was estimated to be around 4.55 eV, which was calibrated by measuring an Ag reference. The material VB was determined using a UV light excitation source (D2) and by extrapolating to zero the cube root of the photoemission signal. The surface morphology and crystal structure of the perovskite films were investigated by field emission scanning electron microscopy (SEM) (JEOL 7000F). The X-ray photoelectron spectroscopy (XPS) measurements were carried out using a SPECS system equipped with a Phoibos 1D-DLD hemispherical energy analyzer. The Al $\alpha$  X-Ray line was used to acquire the spectra and the spectra were references by the C1s peak at 248.8 eV. The PSCs were evaluated under an inert atmosphere using an ABB solar simulator (Sol1A, Oriel), equipped with a 450 W Xe lamp and an AM1.5G filter. The intensity was calibrated at  $100 \text{ mW cm}^{-2}$  using a KG5 windowed Si reference cell. The J–V curves were recorded at a constant scan rate of  $20 \text{ mV s}^{-1}$  using a multiplexor test board system (Ossila), and no device preconditioning was applied prior to measurements. During each measurement, a black metallic aperture mask was used to set the active area of the manufactured devices at  $0.04 \text{ cm}^2$  and to reduce the influence of scattered light. For the long-term lifetime measurements, the devices were transferred to the testing chamber ISOSun (InfinityPV) where they were exposed to continuous illumination of 1 sun and a temperature above  $65 \text{ }^{\circ}\text{C}$ . The relative humidity was around 15–25%. The apparatus was equipped with a solar simulator using a metal halide source simulating the AM1.5G spectrum in the range 300–900 nm. The light intensity was calibrated at  $100 \text{ mW cm}^{-2}$  using a Si reference cell. The devices were maintained at open circuit between lifetime measurements.

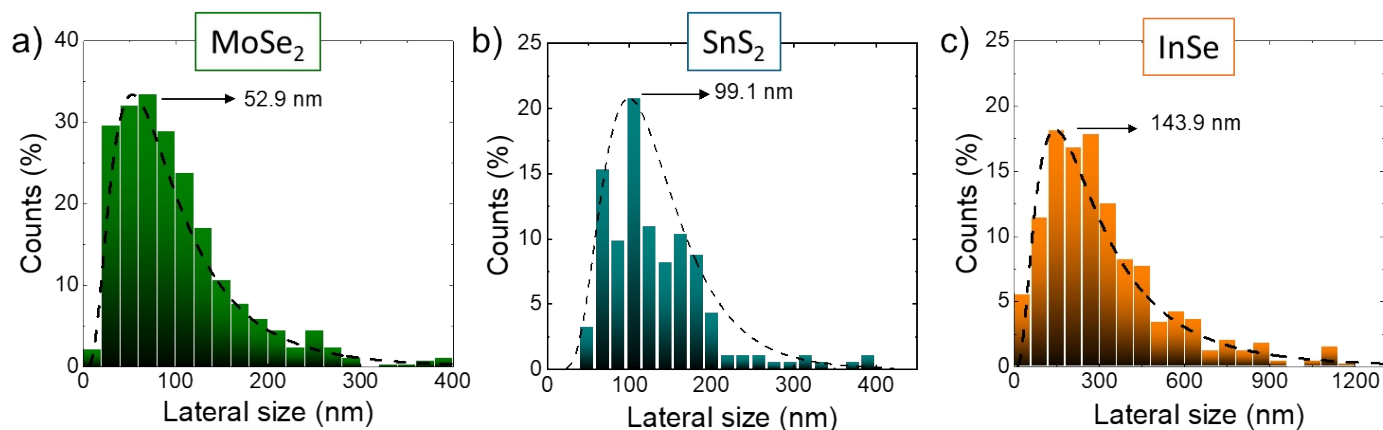


**Figure S1.** Statistical TEM analysis of the lateral size of a)  $\text{MoSe}_2$ , b)  $\text{SnS}_2$  and c)  $\text{InSe}$  nanosheets.

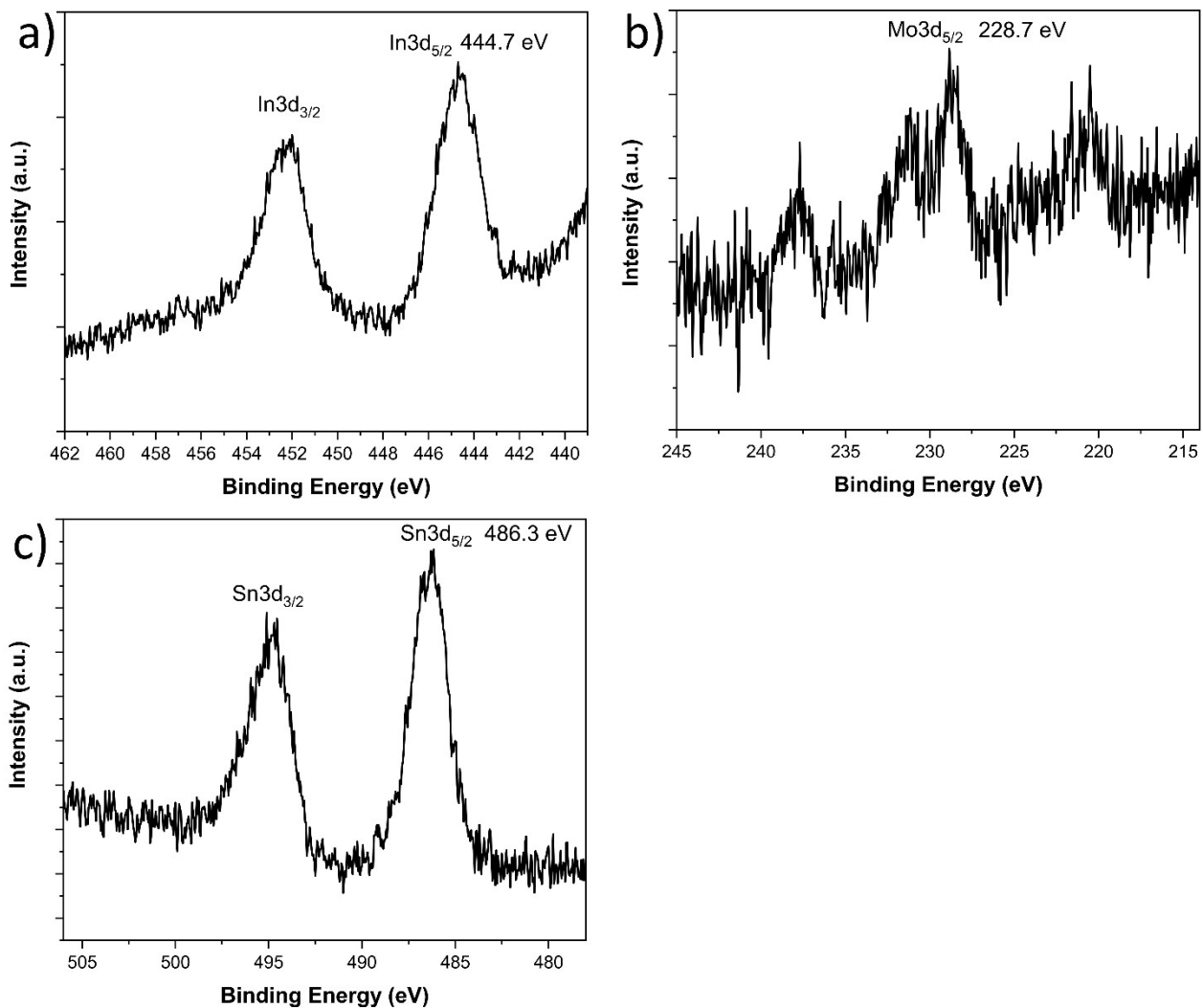


**Figure S2.** XPS spectra of a) InSe (In3d region), b) MoSe<sub>2</sub> (Mo3d region), and c) SnS<sub>2</sub> (Sn3d region) interlayers, deposited atop the perovskite

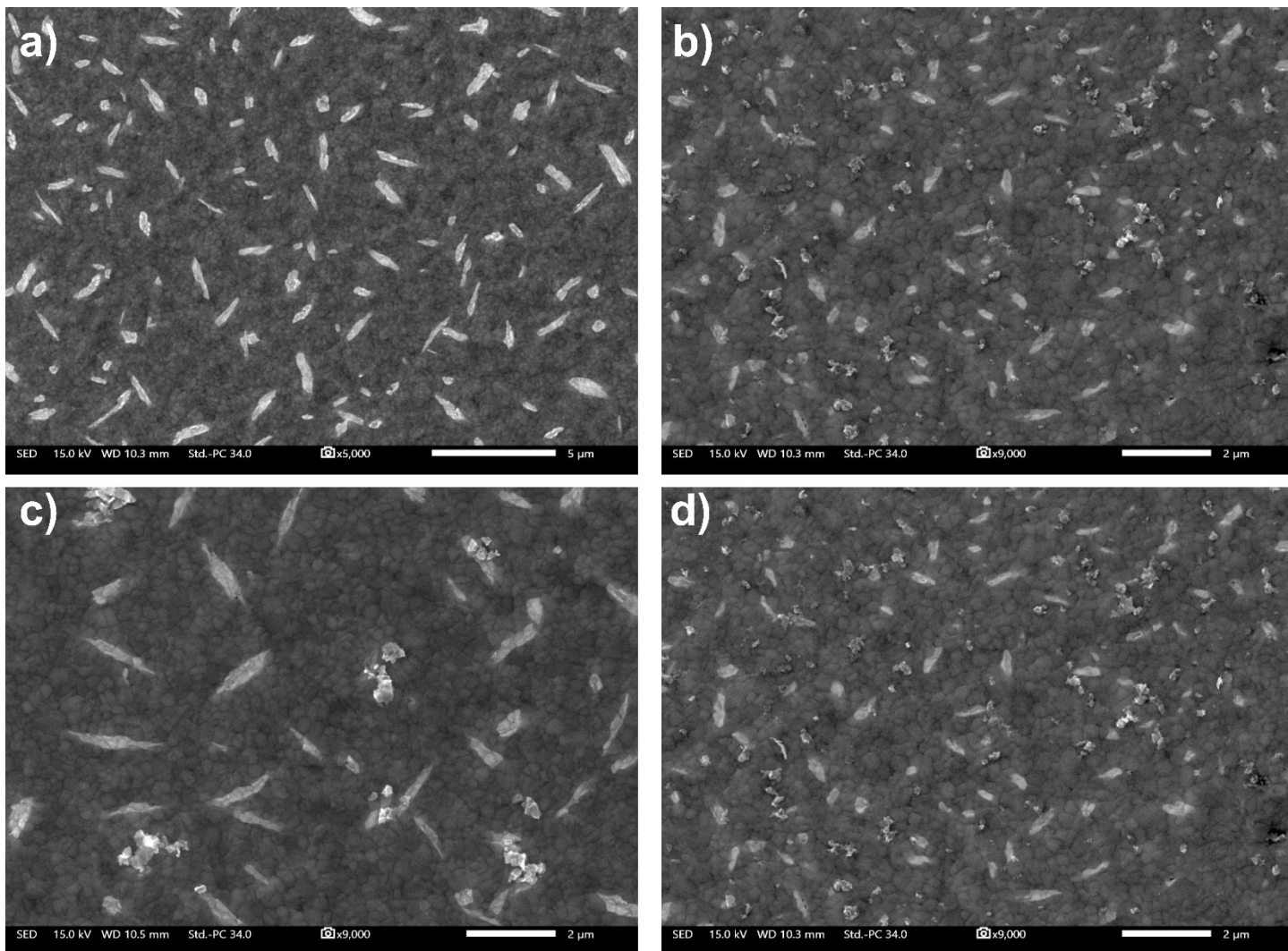


**Figure S3.** Top-view SEM images of a) perovskite surface b) SnS<sub>2</sub>, c) InSe, and d) MoSe<sub>2</sub> interlayers deposited atop the perovskite.

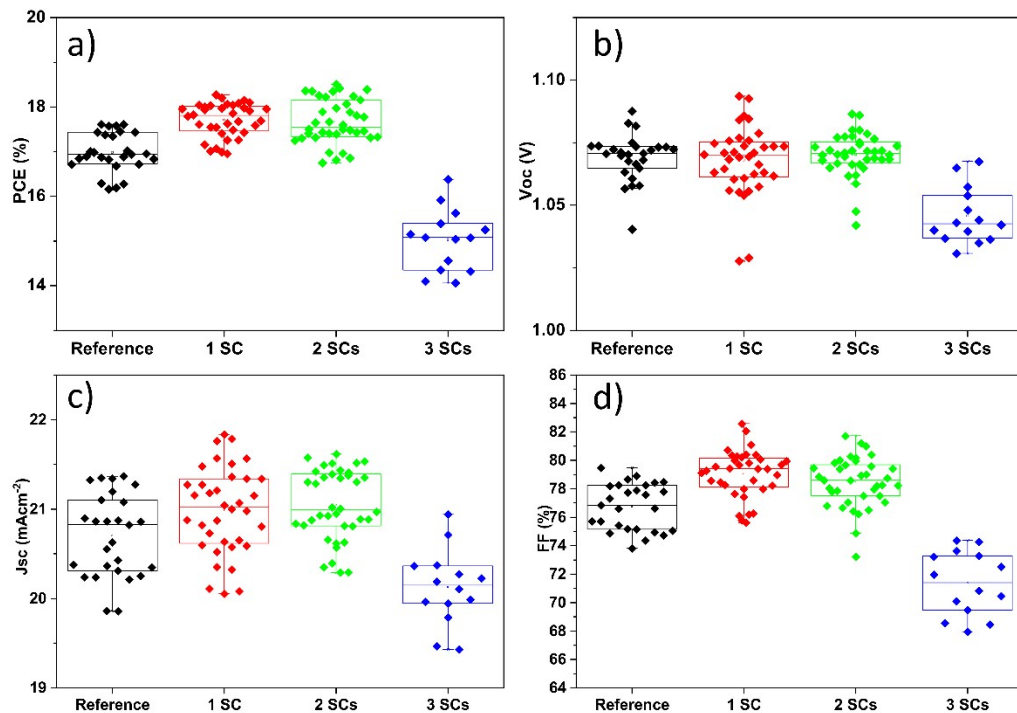


**Figure S4.** Box charts showing the photovoltaic parameters a) PCE, b)  $V_{oc}$ , c) FF, and d)  $J_{sc}$  for the SnS<sub>2</sub>-incorporating devices as a function of successive spin coatings (SCs) of the SnS<sub>2</sub> dispersion.

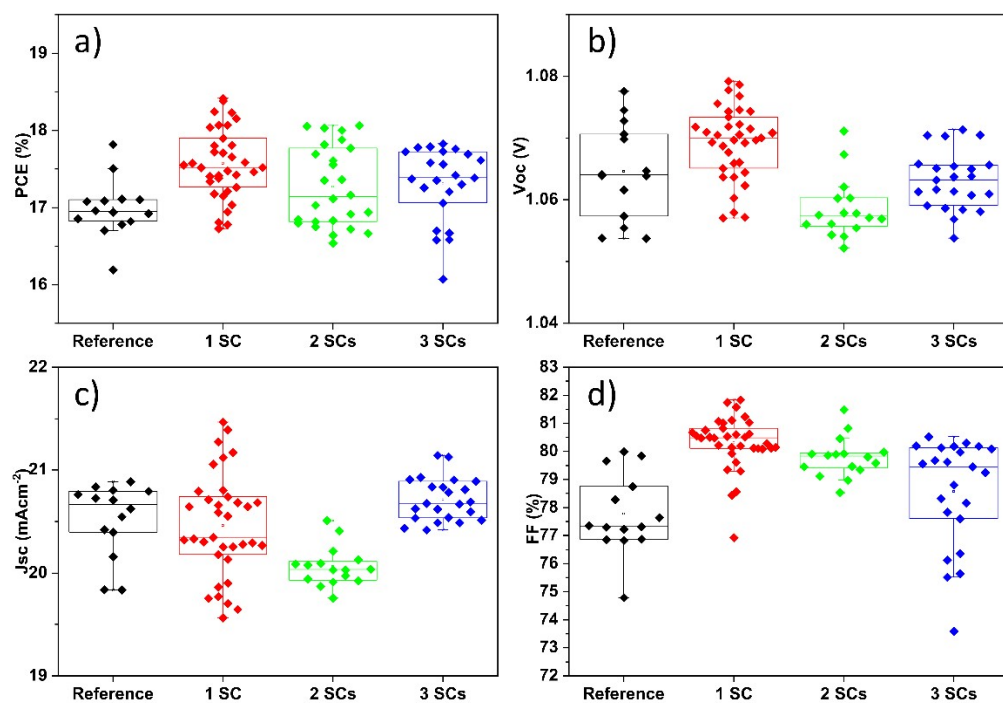


**Figure S5.** Box charts showing the photovoltaic parameters a) PCE, b)  $V_{oc}$ , c) FF, and d)  $J_{sc}$  for the InSe-incorporating devices as a function of successive SCs of the InSe dispersion.

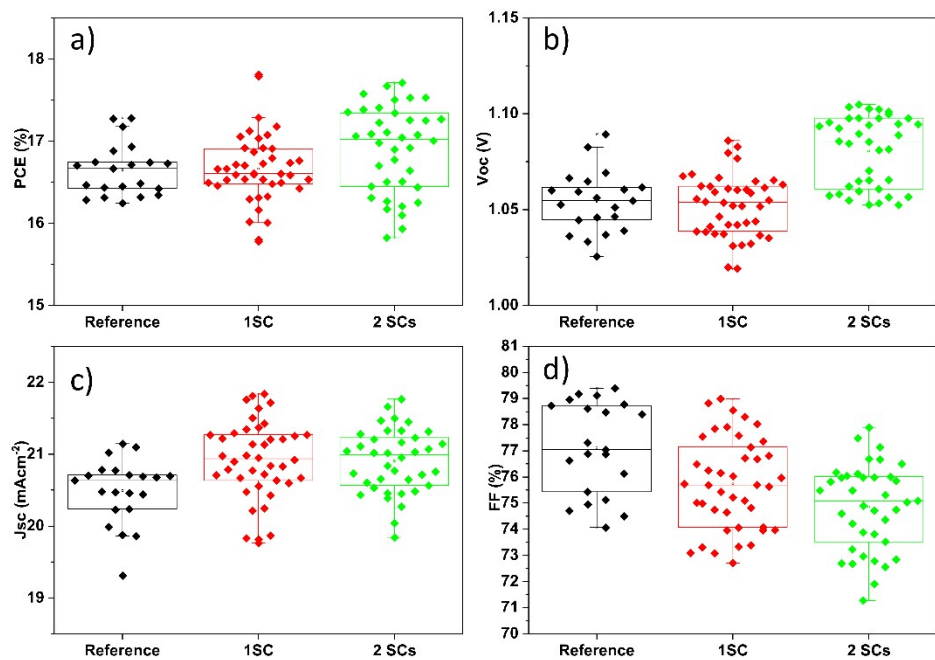


**Figure S6.** Box charts showing the photovoltaic parameters a) PCE, b)  $V_{oc}$ , c) FF, and d)  $J_{sc}$  for the MoSe<sub>2</sub>-incorporating devices as a function of successive SCs of the MoSe<sub>2</sub> dispersion.

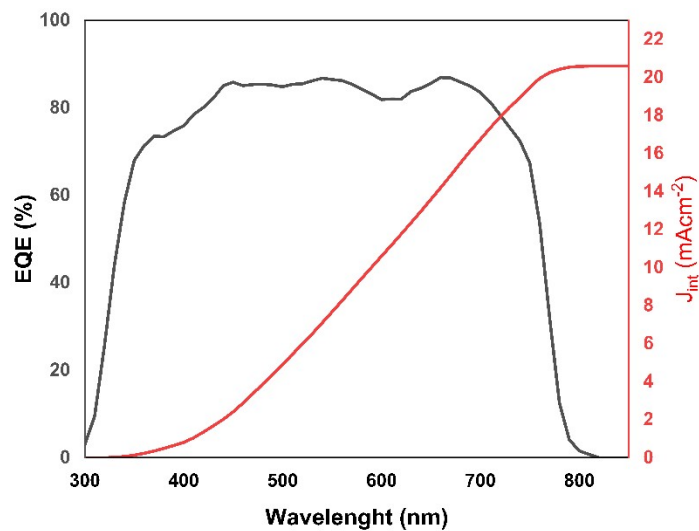


**Figure S7.** External quantum efficiency spectrum of the best performing device and the calculated integrated current  $J_{int}$ .

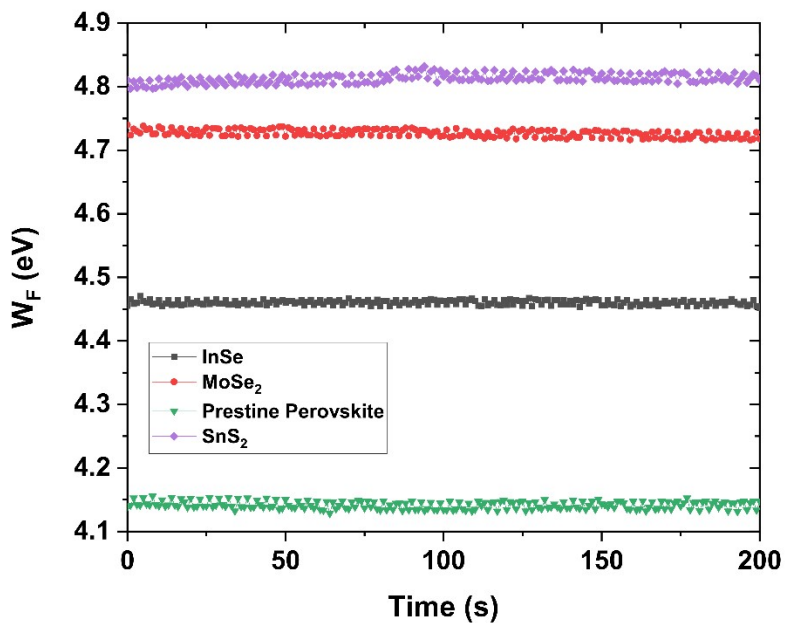


**Figure S8.** Stabilized  $W_F$  measurements of the perovskite surface and TMC interlayers deposited atop the perovskite.

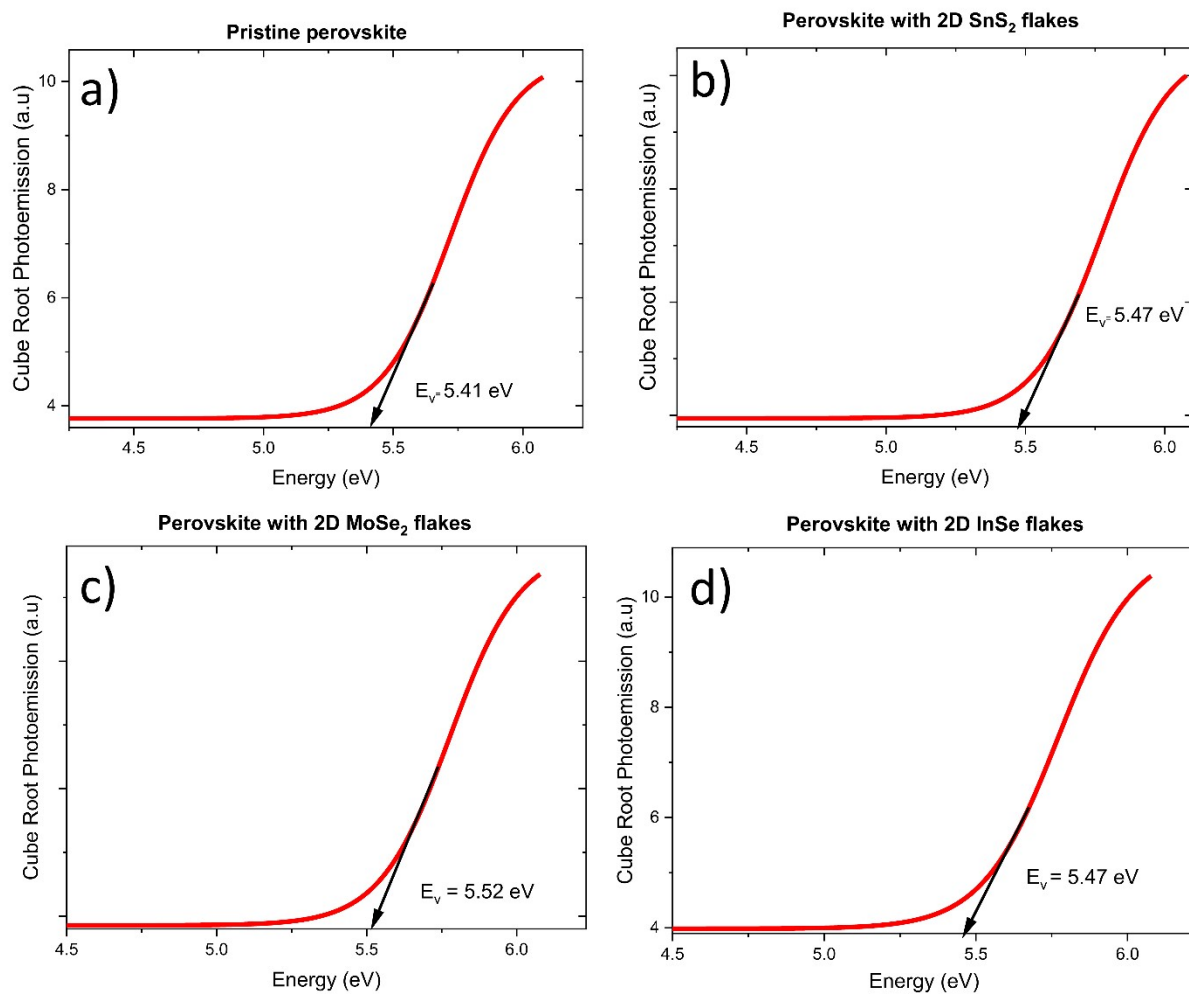


**Figure S9.** APS measurements of perovskite and 2D TMC interlayer deposited atop the perovskite.

## References

- <sup>1</sup> B. Gürbulak, M. Şata, S. Dogan, S. Duman, A. Ashkhasi, and E.F. Keskenler, “Structural characterizations and optical properties of InSe and InSe:Ag semiconductors grown by Bridgman/Stockbarger technique,” *Physica E: Low-Dimensional Systems and Nanostructures* **64**, 106–111 (2014).
- <sup>2</sup> G. Bianca, M.I. Zappia, S. Bellani, M. Ghini, N. Curreli, J. Buha, V. Galli, M. Prato, A. Soll, Z. Sofer, G. Lanzani, I. Kriegel, and F. Bonaccorso, “Indium Selenide/Indium Tin Oxide Hybrid Films for Solution-Processed Photoelectrochemical-Type Photodetectors in Aqueous Media,” *Advanced Materials Interfaces* **10**(1), 2201635 (2023).
- <sup>3</sup> C. Backes, A.M. Abdelkader, C. Alonso, A. Andrieux-Ledier, R. Arenal, J. Azpeitia, N. Balakrishnan, L. Banszerus, J. Barjon, R. Bartali, S. Bellani, C. Berger, R. Berger, M.M.B. Ortega, C. Bernard, P.H. Beton, A. Beyer, A. Bianco, P. Bøggild, F. Bonaccorso, G.B. Barin, C. Botas, R.A. Bueno, D. Carriazo, A. Castellanos-Gomez, M. Christian, A. Ciesielski, T. Ciuk, M.T. Cole, J. Coleman, C. Coletti, L. Crema, H. Cun, D. Dasler, D. De Fazio, N. Díez, S. Drieschner, G.S. Duesberg, R. Fasel, X. Feng, A. Fina, S. Forti, C. Galiotis, G. Garberoglio, J.M. García, J.A. Garrido, M. Gibertini, A. Götzhäuser, J. Gómez, T. Greber, F. Hauke, A. Hemmi, I. Hernandez-Rodriguez, A. Hirsch, S.A. Hodge, Y. Huttel, P.U. Jepsen, I. Jimenez, U. Kaiser, T. Kaplas, H. Kim, A. Kis, K. Papagelis, K. Kostarelos, A. Krajewska, K. Lee, C. Li, H. Lipsanen, A. Liscio, M.R. Lohe, A. Loiseau, L. Lombardi, M. Francisca López, O. Martin, C. Martín, L. Martínez, J.A. Martín-Gago, J. Ignacio Martínez, N. Marzari, Á. Mayoral, J. McManus, M. Melucci, J. Méndez, C. Merino, P. Merino, A.P. Meyer, E. Miniussi, V. Miseikis, N. Mishra, V. Morandi, C. Munuera, R. Muñoz, H. Nolan, L. Ortolani, A.K. Ott, I. Palacio, V. Palermo, J. Parthenios, I. Pasternak, A. Patane, M. Prato, H. Prevost, V. Prudkovskiy, N. Pugno, T. Rojo, A. Rossi, P. Ruffieux, P. Samorì, L. Schué, E. Setijadi, T. Seyller, G. Speranza, C. Stampfer, I. Stenger, W. Strupinski, Y. Svirko, S. Taioli, K.B.K. Teo, M. Testi, F. Tomarchio, M. Tortello, E. Treossi, A. Turchanin, E. Vazquez, E. Villaro, P.R. Whelan, Z. Xia, R. Yakimova, S. Yang, G.R. Yazdi, C. Yim, D. Yoon, X. Zhang, X. Zhuang, L. Colombo, A.C. Ferrari, and M. Garcia-Hernandez, “Production and processing of graphene and related materials,” *2D Materials* **7**(2), 022001 (2020).
- <sup>4</sup> E. Petroni, E. Lago, S. Bellani, D.W. Boukhvalov, A. Politano, B. Gürbulak, S. Duman, M. Prato, S. Gentiluomo, R. Oropesa-Nuñez, J.-K. Panda, P.S. Toth, A.E. Del Rio Castillo, V. Pellegrini, and F. Bonaccorso, “Liquid-Phase Exfoliated Indium–Selenide Flakes and Their Application in Hydrogen Evolution Reaction,” *Small* **14**(26), 1800749 (2018).